

Authentication Security of PRF GNSS Ranging

Jason Anderson, *Xona Space Systems*

Abstract—This work derives the authentication security of pseudorandom function (PRF) GNSS ranging under multiple GNSS spoofing models, including the Security Code Estimation and Replay (SCER) snooper. When GNSS ranging codes derive from a PRF utilizing a secret known only to the broadcaster, the snooper cannot predict the ranging code before broadcast. Therefore, PRF ranging can be used to establish trust in the GNSS pseudoranges and the resulting receiver position, navigation, and timing (PNT) solution. I apply the methods herein to Galileo’s Signal Authentication Service (SAS) utilizing the encrypted Galileo E6-C signal to compute that, at most, 400 ms of Galileo E6-C data to assert 128-bit authentication security under non-SCER models. For the SCER adversary, I predict the adversary’s needed receiving radio equipment to break authentication security. One can use this work to design a PRF GNSS ranging protocol to meet useful authentication security requirements by computing the probability of missed detection. Receivers can use the techniques in this work to mathematically bound and improve the sensitivity and specificity of their authentication processing.

Index Terms—GNSS Authentication, Navigation Security, TESLA

I. INTRODUCTION

CRYPTOGRAPHIC authentication for satellite navigation ranging is progressing quickly from concept to real-world deployment. Galileo Signal Authentication Service (SAS) started in orbit testing with encrypted E6-C signals [1], [2]. And, Xona Space Systems broadcast its first watermarked signal in July 2025 [3]. This work comes just in time as Global Navigation Satellite System (GNSS) signal spoofing becomes a common nuisance in conflict zones and nearby public infrastructure.

GNSS signals typically provide two signal component types: data and ranging. Data components typically provide information related to broadcasting satellites’ position and clock bias. Ranging components enable receivers to measure their range to satellites by transmitting a high-auto-correlative, low-cross-correlative ranging code. These two components together enable receivers to solve a trilateration problem to deduce their position and time. Cryptographic ranging authentication involves augmenting the ranging components with cryptographic elements [4]. The cryptographic construction asserts that these elements are not predictable by GNSS spoofers before broadcast. When a receiver observes these cryptographic elements, it establishes trust in the measured pseudoranges that determine the receiver’s position and time.

Cryptographic ranging authentication comes in two forms. The first involves inducing a watermark within the ranging code [3], [5]. The watermark enacts a cryptographic perturbation on the ranging code chips¹ that is designed to be small.

Manuscript received October ??, 2025; revised October ??, 2025.

¹Each bit in a GNSS ranging code is called a chip rather than a bit.

And because the watermark is a small perturbation, receivers can still track the signal and ignore the watermark’s existence. The second form of cryptographic ranging authentication requires the entire ranging code derive from a cryptographic Pseudorandom Function (PRF). When the ranging code is a PRF, receivers cannot track the signal until they have the cryptographic seeds used to generate the PRF ranging code.

Both watermark and PRF ranging authentication systems enact a bit-commitment authentication protocol, usually under a Timed Efficient Stream Loss-tolerant Authentication (TESLA) framework [6]. Xona’s Pulsar, GPS’s Chimera, and Galileo’s SAS will utilize TESLA [1], [3], [7]. The authentication procedure can be briefly summarized as follows. First the GNSS provider commits to a secret from which the watermarked or the PRF ranging code derives. Second, after a delay, the GNSS provider will reveal that commitment secret to receiver. Third, the receiver can retrieve the corresponding radio measurements in the past and process the watermark or PRF ranging code to determine a pseudorange’s authenticity utilizing the revealed secret.

For a cryptographic ranging authentication system to be useful, there must be a receiver signal processing procedure that is sensitive and specific. The probability a snooper could produce a signal that would fool a receiver authenticity determination, called the Probability of Missed Detection (PMD), must be small. Moreover, the probability an authentic signal would raise an alarm, called the Probability of False Alarm (PFA), must also be small. For the watermark case, when the watermark is a Combinatorial Watermark, there exists a receiver processing procedure that can compute the PMD and PFA and then assert cryptographic authentication security [8]. With the mathematical PMD and PFA models, the watermark degradation can be minimized while achieving security levels of standard cryptographic guidelines.

For the PRF case, this work provides the equivalent to that provided for Combinatorial Watermark ranging by [8], [9], [10]. Several works propose receiver processing statistics based on the pseudorange differences between authenticating PRF pseudoranges and non-authenticated pseudoranges to authenticate the non-authenticated pseudoranges [2], [11]. However, environmental effects unrelated to spoofing threats interfere with this methodology’s specificity (i.e., the observed PFA), nor do they provide mathematical proof of security by bounding the PMD. Previous work utilized statistic arguments on multiple chip measurements [12], [13]. However, they do not exploit the relationship among many unpredictable chips and the quickly-decaying tails of the binomial distribution to provide mathematical arguments of the levels of standard cryptographic security. After asserting standard cryptographic security levels utilizing this work, receiver thresholds on pseudorange differences can be expanded to increase the processing

specificity without compromising security.

This work provides a signal processing procedure and demonstrates how to bound the PMD and PFA of receiver statistics of PRF ranges to standard cryptographic security levels (e.g., 128-bit security). I apply multiple security models to these security claims and provide simulated results of adversary capabilities. The principal mathematical results are each verified with Monte Carlo experiments. And each of the results are applied to Galileo's SAS with Galileo's E6-C service, an upcoming PRF ranging authentication provider.

A. PRF Ranging

GNSS ranging codes are designed to have high autocorrelation and low cross-correlation. The receiver will use a replica of the ranging code to shift-correlate with its observed radio signal. The high autocorrelation enables the receivers to lift the signal from the noise, and the sharp autocorrelation peak enables the receiver to measure a precise signal arrival time forming a pseudorange. At least four satellite pseudoranges enable a receiver to deduce its position and time via trilateration.

Random codes can serve as ranging codes since random sequences have high autocorrelation and low cross-correlation. Moreover, pseudorandom code sequences, sequences that appear random but actually derive from a deterministic process, also suffice. When a ranging code derives from a cryptographic PRF, the ranging code inherits cryptographic security properties. For instance, when a ranging code derives from a cryptographic PRF utilizing a secret seed, then the ranging code admits no efficient algorithm that can distinguish it from a truly random sequence nor predict future chips with probability better than random guessing. Before a PRF ranging code's broadcast, their security limits adversarial attempts to forge ranging signals to that of random guesses. PRF ranging codes can be derived multiple ways, including via encryption or cryptographic hashing. PRF ranging exists in practice today with encrypted GNSS signal's such as GPS's M-Code and Galileo's PRS.

Galileo's SAS will enact PRF ranging authentication with Galileo's encrypted E6-C signal with assistance from Galileo's Open Service Navigation Message Authentication (OSNMA) on Galileo's E1-B signal [14], [15]. The design can be summarized as follows. Galileo will encrypt the ranging codes of its E6-C signal and never disclose the deriving key. Galileo will perform a second encryption on the E6-C ranging codes utilizing the undisclosed TESLA keys from OSNMA. These second-encrypted ranging codes will be available for download from a server to any receiver. As OSNMA reveals TESLA keys, the receiver will be able decrypt the second-encrypted E6-C ranging codes and perform post processing of the E6-C signal to determine authenticity. Receivers can utilize the derivations and procedures of this work to determine authenticity with high confidence.

B. Chip Estimation Theory

Ranging signals can be modeled as binary keyed code, usually Binary Phase-Shift Keyed (BPSK). Each broadcast bit,

mapped to -1 or 1 , is called a chip. When the ranging code derives from a PRF, the adversary cannot predict the chips before their broadcast. But some adversaries considered in section I-D can measure the chips after broadcast. Typically, GNSS ranging signals are below the thermal noise floor, which makes measuring individual chips difficult without large directional antenna.

Given the noise power σ^2 and the signal power P , a single measurement of the BPSK baseband (i.e., after carrier removal) signal S is

$$N \sim \mathcal{N}(0, \sigma^2); \quad (1)$$

$$S = \pm\sqrt{P} + N. \quad (2)$$

With this model, the probability of successfully measuring a chip correctly p is

$$p = \text{cdf}_N\left(\sqrt{P}\right). \quad (3)$$

This chip estimation model is simple but effective, serving the purposes of this work.

C. GNSS Signal and Receiver Processing Models

GNSS signals typically involve a baseband signal modulated with a carrier wave. They are also typically subdivided into a discrete ranging code units, for which we let n be the number of chips per unit and T be time length per unit. For instance, Galileo E6-C utilizes $n = 5115$ chip ranging codes that repeat every $T = 1$ ms. Each millisecond ranging code within Galileo E6-C can become a PRF ranging code at will when encryption is turned on.

The mathematics of this work begin after the receiver has removed the carrier wave with a tracking loop. Later in this section, I discuss how I account for the effect of tracking errors. Therefore, let the GNSS authentic baseband signal be

$$S^{\text{auth}} = \sqrt{P}R^{\text{PRF}} + N. \quad (4)$$

In eq. (4), S , R , and N are each vectors that span a single ranging code. When the receiver sampling frequency is F , then the length of each is FT . $R^{\text{PRF}} \in \{-1, 1\}^{FT}$ is the resampled *replica* of the PRF sequence. P is the power of the signal, which for now is constant per ranging code, but this assumption is relaxed in section V-A.

Figure 1 provides a block diagram of a radio performing the authentication determination. Within the gray box of fig. 1 exists a standard GNSS tracking loop where, after carrier removal, multiple replica correlations aid a tracking loop. Initially, the receiver will not have knowledge of R^{PRF} , so it must receive the authenticated tracking states from a network or by tracking another synchronized signal. For instance, with Galileo's SAS, the Galileo's encrypted E6-B and Galileo's open E1-B signal can initially be used for tracking before observing the encrypted E6-C after the PRF secrets are revealed. Because Galileo's E6-B is transmitted on the same band as E6-C (as opposed to Galileo's E1-B), utilizing Galileo's E6-B tracking states will not need corrections related to the signal carrier (assuming, reasonably, Galileo can transmit E6-B and E6-C with a fixed phase delay perfectly). Before the receiver

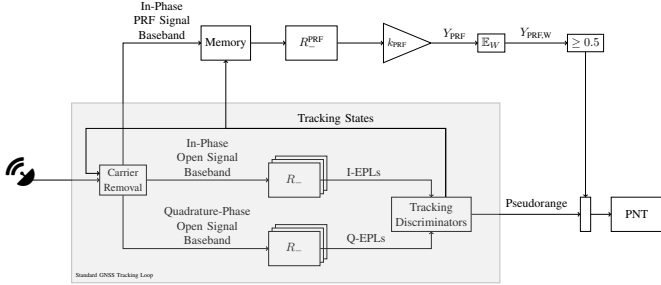


Fig. 1. An example radio block diagram that describes how PRF ranging would occur. The gray box diagrams a typical tracking loop where early, prompt, and late (EPL) correlations are used to form a tracking loop to determine the carrier phase, doppler, and code phase. An unknown PRF sequence is known to be present, so the baseband samples are stored into memory awaiting the PRF replica seed. After distribution of the PRF seed, the receiver will do an additional correlation with the PRF replica to determine authenticity. This figure depicts the case where a PRF signal is used to authenticate another signal: like if the encrypted Galileo E6-C is used to authenticate the open Galileo E1-B. A similar authentication system could use the PRF ranges directly for Position, Navigation, and Timing (PNT).

gets the needed secrets to derive R^{PRF} within the E6-C signal, the receiver must store the baseband samples in memory.

After the receiver derives R^{PRF} , it can process those stored baseband samples to determine authentication. Within fig. 1, the samples from memory are fed into an linear time-invariant (LTI) matching filter R^{PRF} , then the gain from eq. (5), then an averaging filter (averaging the result of W ranging codes), and then finally a threshold gate that determines authenticity.

$$k_{\text{PRF}} = \frac{1}{\|R^{\text{PRF}}\|_1} \frac{1}{\sqrt{P}} = \frac{1}{FT} \frac{1}{\sqrt{P}} \quad (5)$$

The construction of filter and gain from fig. 1 was judiciously chosen to enable a concise mathematical pathway to bound the PMD and PFA, which will be apparent later.

Implicit in the filter gain from eq. (5) is that the radio has a secure way (i.e., resistant to adversarial manipulation) to determine the power of the incoming signal. In this work, I adopt the argument from [8] by assuming that that a receiver will cease to function and will not attempt to authenticate when the $C/N_0 < 30$ dB-Hz. Typical receivers coherently integrating over $T = 1$ ms will need much larger C/N_0 , meaning that 30 dB-Hz is meant to an unreasonably low worst case. So throughout this work, I assume that the receiver will cease making an authentication determination if the measured $C/N_0 < 30$ dB-Hz. For the security derivations, I assume that $C/N_0 = 30$ dB-Hz. Because assuming this unfavorable noise condition makes the security results worse, the receiver should expect better security in reasonable operating conditions. But by selecting this conservative value, I claim that I account for the uncertainty resulting from an adversary manipulating the receiver's power estimator, simultaneously jamming the receiver, or inducing tracking errors.

Similarly, when forming a radio model useful for making authentication security arguments, it is appropriate to form a conservative, worst-case receiver radio model. For this work, I assume that the radio operates at the Nyquist Frequency (in addition to the unreasonable C/N_0 from the previous paragraph). For instance, for Galileo's E6-C, $F = 10.230$ MHz.

Notation	Definition and Short Description
n	The number of chips within a single ranging code (or ranging code segment). For instance, for Galileo's E6-C, $n = 5115$.
T	The length of time covering a single ranging code. For instance, for Galileo's E6-C, $T = 1$ ms.
W	The number of ranging codes (or ranging code segments) that should be aggregated when making an authentication determination.
R	A replica of the ranging code with elements -1 and 1 , sometimes with a superscript denoting what generated the replica and subscript denoting whether it is reversed in time for a matching convolution.
F	The sampling rate of the radio making the authentication determination.
S	The signal measured over T with frequency F .
P	The power of the ranging signal immediately preceding correlation.
σ^2	The noise power immediately preceding correlation.
p	The probability of correctly estimating a chip.

TABLE I
NOTATION TABLE

Again, one should expect better-reported-security for a real receiver out in the field because they will utilizing a sampling frequency greater than the required Nyquist frequency.

Table I provides a notation table for the reader's convenience.

D. Adversarial Models

To begin defining the adversarial models of this work, first consider a simple GNSS spoofer with only a transmitting antenna for an open (i.e., not encrypted) signal. This adversary has access to the signal specification, and the ranging signal is simply a repeated, known ranging code. So the adversary can utilize the specification to submit forged signals to the receiver. To manipulate the victim's deduced position and time, the adversary manipulates the arrival times of the forged signals. Now suppose the spoofed signal derives from a PRF derived from a secret unknown to anyone except the GNSS provider. Without the needed cryptographic secrets, the adversary cannot predict the ranging codes before the GNSS provider broadcasts them, even with possession of the signal specification. However, a GNSS spoofer with listening and transmitting antenna could observe and then replay the PRF sequence to the victim receiver.

There exists a breadth of GNSS spoofing adversarial models, but for this work there is a useful binary classification. For this work, the adversary either engages in a Security Code Estimation and Replay (SCER) or it does not [12]. In an SCER attack, the adversary attempts to observe the unpredictable chips before submitting a forgery to the victim receiver. When the receiver does not engage in an SCER attack, it is called a Non-SCER adversary. This binary classification poses a convenience for the mathematical derivations of this work.

1) *Non-SCER*: The Non-SCER adversary makes no attempt to observe the cryptographic PRF ranging codes before submitting a signal to the victim receiver. Therefore, were the Non-SCER adversary to submit a spoof of the form of eq. (4), it must guess its own replica:

$$S^{\text{-SCER}} = \sqrt{P} R^{\text{-SCER}} + N \quad (6)$$

Suppose the Non-SCER adversary elects to manipulate the authentic signal by adding another noise term of a distribution unknown to the receiver. When the ranging signal is fed through the authentication filter, which is a match filter, the output enacts what amounts to an averaging filter with typically a large number of samples. For instance, for Galileo's E6-C, this will amount to at least $FT = 10230$ samples. Moreover, the output of the match filter will be averaged at least $W = 100$ more times thereafter. When this unknown distribution is independent and identically distributed (IID) and has finite variance, then this distribution will suffer Central Limit Theorem (CLT) effects through this filter to produce something that approaches a normal distribution anyway. Similarly, were the Non-SCER adversary to submit a spoof of the form of eq. (6) but vary the power, this would in effect add another unknown noise distribution that approaches a normal distribution after filtering. If such manipulation were to provide an advantage in increasing the correlation within the match filter, the adversary would have an efficient algorithm that predicts the output of the deriving PRF. But since the PRF asserts that impossible, Non-SCER power manipulation poses no advantage.

Now one could question these assumptions over authentication determinations that involve more than 1 million samples. However, for this work, the Non-SCER adversary has no advantage with manipulating P over time nor adding another non-normal noise term. So for this work, the Non-SCER adversary will submit a spoof of the form of eq. (6) with constant P and noise N . Without any way to predict R^{PRF} , R^{SCER} will be a random guess of length n resampled into FT . In this work, I assume the sampling FT uniformly spans n and that the small sampling quantity differences among chips poses no exploitable advantage to the Non-SCER adversary. Again, were there an algorithm that the FT resampling posed an advantage (e.g., the adversary could predict the polarity of the chips with more-than-average-samples-per-chip), then that adversary would break the cryptographic security of the PRF, which the PRF asserts impossible. Moreover, the same argument can be applied to the effect of measurement discretization and the associated gain control before the tracking loop.

Utilizing the Non-SCER adversarial model, I show how to bound PMD and PFAs for PRF ranging authentication schemes.

2) *SCER*: The SCER adversary uses receiving antenna to estimate R^{PPF} before submitting to its victim receiver. Because the adversary has access to measurements of R^{PPF} , the SCER adversary should have a better-than-50% chance of guessing each chip, so cryptographic arguments will not be as helpful. As the SCER adversary utilizes better equipment, that probability will increase until it can perfect estimate the individual chips and completely break the ranging authentication security. Unfortunately, cryptography is not useful for protecting against delays and delays affect the receiver's deduced PNT, so cryptographic security will not be obtainable for the SCER case. However, the argument can be offloaded on to whether the receiver can reject late signals and whether authorities can detect SCER receiving antenna under their jurisdiction.

There are two principle ways to limit the effectiveness of

SCER adversaries. The first principle way exploits how an SCER adversary must submit its spoof to the victim after a delay. It requires time for the SCER to observe the R^{PPF} , process its measurements, and transport its forgery to the victim receiver. Even with a no-latency SCER model, there is a fundamental limitation via speed of light. Therefore, the receiver can reject SCER-spoofed signals by rejecting late signals. For the purpose of this method, the receiver cannot use the timing solution provided by GNSS or any other broadcast-only signal [16]. This means that the receiver must utilize a GNSS-Independent clock to reject late signals. Then the challenge is the accuracy of this GNSS-independent clock: a nanosecond of uncertainty can mean about 3 meters of position uncertainty, which is not helpful or considered for this work.

Instead, the second principle way exploits the low-power nature of the ranging signal. As the power of the signal decreases, the adversary's chip estimation process becomes more difficult, for which the adversary can compensate by increasing the effectiveness of its radio equipment. However, the adversary cannot increase the effectiveness of its radio equipment indefinitely without detection. As the signal's power decreases and the required SCER equipment increases, it should be easier for authorities on the ground to observe and destroy SCER spoofers.

The mathematical derivations of this work utilize a limited SCER adversary called the Hard-decision SCER (HDSER) adversary. The HDSER adversary utilizes section I-B to make hard decisions on each measured chip, ignoring potentially useful soft information (e.g., the posterior probability of the chip measurement). Since the HDSER's only advantage over the Non-SCER is a p -accurate hard-decision estimate of the PRF ranging code, there is no still advantage in changing the power. Limiting to the HDSER adversary will yield useful mathematically concise predictions similar to those by the Non-SCER adversary. Sadly, I am unaware of how to concisely extend the derivations herein to an SCER adversary that utilizes soft information. However, this assumption is relaxed in section V-A, where I show a simple soft-information-using SCER from [8], [13], called PSCER, that demonstrates a small advantage to the HDSER that manipulates the individual chip powers. This small advantage can be accounted for by adjusting the results of the HDSER. There could be other soft-information adversaries that could do better. However, we approach the universal trade between an approximate problem with an exact solution versus an exact problem with an approximate solution.

Utilizing the mathematical derivations for the HDSER case, and the results from the PSCER case, I show how to predict the needed adversarial radio equipment, which would be useful to communicate to authorities on the ground so they know what to search for and destroy.

II. PROBABILITY OF FALSE ALARM

To derive the PFA in the authentic for the threshold statistic from fig. 1, let the authentic signal be

$$S^{\text{auth}} = \sqrt{P}R^{\text{PRF}} + N . \quad (4)$$

Now I feed S^{auth} into the LTI filter R^{PRF} :

$$\begin{aligned} Y_{\text{PRF}} \mid \text{auth} &= k_{\text{PRF}} \cdot R_{-}^{\text{PRF}} * S^{\text{auth}} \\ &= k_{\text{PRF}} \cdot R_{-}^{\text{PRF}} * (\sqrt{P} R^{\text{PRF}} + N) \\ &= k_{\text{PRF}} \sqrt{P} \cdot R_{-}^{\text{PRF}} * R^{\text{PRF}} + k_{\text{PRF}} \cdot R_{-}^{\text{PRF}} * N; \\ Y_{\text{PRF}} \mid \text{auth} &= 1 + k_{\text{PRF}} \cdot R_{-}^{\text{PRF}} * N. \end{aligned} \quad (7)$$

Finally, specifying the distribution is a noise propagation exercise:

$$N_{FT} \sim \mathcal{N} \left(0, \frac{1}{FT} \frac{\sigma^2}{P} \right); \quad (8)$$

$$Y_{\text{PRF}} \mid \text{auth} = 1 + N_{FT}. \quad (9)$$

Because of the low-power nature of GNSS signals, the receiver will need to aggregate many of these statistics. Since eq. (9) presents a normal distribution, taking the average of W simply changes the variance of the noise term:

$$N_{FTW} \sim \mathcal{N} \left(0, \frac{1}{W} \frac{1}{FT} \frac{\sigma^2}{P} \right); \quad (10)$$

$$Y_{\text{PRF},W} \mid \text{auth} = 1 + N_{FTW}. \quad (11)$$

The expectation $Y_{\text{PRF},W} \mid \text{auth}$ is 1. Later, in section III, I derive that the expectation in the Non-SCER spoofing case as 0. Without any reason to favor the PMD or PFA, I select a midpoint threshold of 0.5 for $Y_{\text{PRF},W}$. To compute the PFA,

$$\begin{aligned} \text{PFA} &= \Pr(Y_{\text{PRF},W} < 0.5 \mid \text{auth}) \\ &= \Pr(1 + N_{FTW} < 0.5); \\ \text{PFA} &= \text{cdf}_{N_{FTW}}(-0.5). \end{aligned} \quad (12)$$

In the following section III, I compute the PMD based on the 0.5 threshold and provide a plot like fig. 2 to aid with the selection of W . However, I do not provide such a plot in this section. Because of the expectation symmetry of the 0.5 threshold in the authentic and non-SCER spoofing case, and because the variance increases in the spoofing case, the PFA will always be less than the PMD in this symmetric 0.5 threshold case. In the following section III, I enable one to select W to meet a specific PMD and security level. So I note that, given the construction of this threshold, the PFA will always be a slightly less than the PMD from section III.

III. NON-SCER PRF RANGING SECURITY

To derive the PMD in the Non-SCER case, let the spoofed signal be

$$S^{\text{-SCER}} = \sqrt{P} R^{\text{-SCER}} + N. \quad (6)$$

Before passing $S^{\text{-SCER}}$ through the LTI filter R^{PRF} , it is helpful to understand the result of convolving R_{-}^{PRF} and $R^{\text{-SCER}}$ before either is resampled. Suppose that the adversary guesses every single chip of R^{PRF} incorrectly. Then the convolution of R^{PRF} and $R^{\text{-SCER}}$ is $-n$ (without resampling). When the adversary guesses every chip of R^{PRF} , then they are perfectly correlated. The likelihood that the adversary guesses any chips follows a fair binomial distribution, but with

each chip guessed correctly, the correlation increases by 2. Therefore,

$$B^{\text{-SCER}} \sim \mathcal{B}(n, 0.5); \quad (13)$$

$$R_{-}^{\text{PRF}} * R^{\text{-SCER}} = (-n + 2 \cdot B^{\text{-SCER}}) \frac{FT}{n}. \quad (14)$$

Let

$$g(b) = \frac{1}{n}(-n + 2b). \quad (15)$$

Now, I feed $S^{\text{-SCER}}$ through the LTI filter R^{PRF} :

$$\begin{aligned} Y_{\text{PRF}} \mid \neg\text{SCER} &= k_{\text{PRF}} \cdot R_{-}^{\text{PRF}} * S^{\text{-SCER}} \\ &= k_{\text{PRF}} \cdot R_{-}^{\text{PRF}} * (\sqrt{P} R^{\text{-SCER}} + N) \\ &= k_{\text{PRF}} \sqrt{P} \cdot R_{-}^{\text{PRF}} * R^{\text{-SCER}} + k_{\text{PRF}} \cdot R_{-}^{\text{PRF}} * N; \end{aligned} \quad (16)$$

$$Y_{\text{PRF}} \mid \neg\text{SCER} = g(B^{\text{-SCER}}) + N_{FT}. \quad (17)$$

$Y_{\text{PRF}} \mid \neg\text{SCER}$ is simply the sum of a linearly transformed binomial distribution and the noise-propagated normal distribution.

The receiver will aggregate W of these identically distributed statistics to make an authentication determination. This means that the CLT can aid designing system parameters by providing closed-form expressions of the distributions. After performing a search of system parameters utilizing the CLT, one can then verify the system parameters with the actual distributions.

To compute the $\mathbb{E}[Y_{\text{PRF}} \mid \neg\text{SCER}]$, noting that g is a linear function:

$$\begin{aligned} \mathbb{E}[Y_{\text{PRF}} \mid \neg\text{SCER}] &= \mathbb{E}[g(B^{\text{-SCER}}) + N_{FT}] \\ &= \mathbb{E}[g(B^{\text{-SCER}})] \\ &= g(\mathbb{E}[B^{\text{-SCER}}]) \\ &= g\left(\frac{n}{2}\right) \\ \mathbb{E}[Y_{\text{PRF}} \mid \neg\text{SCER}] &= 0. \end{aligned} \quad (18)$$

And to compute the variance:

$$\begin{aligned} \mathbb{V}[Y_{\text{PRF}} \mid \neg\text{SCER}] &= \mathbb{V}[g(B^{\text{-SCER}}) + N_{FT}] \\ &= \mathbb{V}[g(B^{\text{-SCER}})] + \mathbb{V}[N_{FT}] \\ &= \mathbb{V}[g(B^{\text{-SCER}})] + \frac{1}{FT} \cdot \frac{\sigma^2}{P} \\ &= \frac{4}{n^2} \mathbb{V}[B^{\text{-SCER}}] + \frac{1}{FT} \cdot \frac{\sigma^2}{P} \\ &= \frac{4}{n^2} \frac{n}{4} + \frac{1}{FT} \cdot \frac{\sigma^2}{P} \\ \mathbb{V}[Y_{\text{PRF}} \mid \neg\text{SCER}] &= \frac{1}{n} + \frac{1}{FT} \cdot \frac{\sigma^2}{P}. \end{aligned} \quad (19)$$

Recall from section II that $\mathbb{E}[Y_{\text{PRF}} \mid \text{auth}] = 1$. Without any reason to favor the PFA and the PMD, I set the authentic versus spoof threshold at $Y = 0.5$. Now the goal should be to find system parameters with an acceptably PMD (noting from section II, that the PFA will be slightly less than the PMD).

The expectation and variance of Y_{PRF} will be useful in performing an efficient search over W to find candidate with a potentially acceptable PMD by employing the CLT. But after

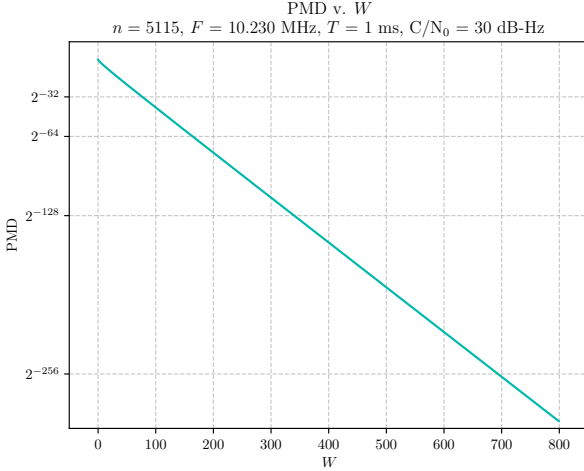


Fig. 2. The PMD computed via eq. (21).

this search, one must directly compute the PMD to verify authentication security. To compute the exact PMD, let

$$B^{-\text{SCER},W} \sim \mathcal{B}(nW, 0.5). \quad (20)$$

Then,

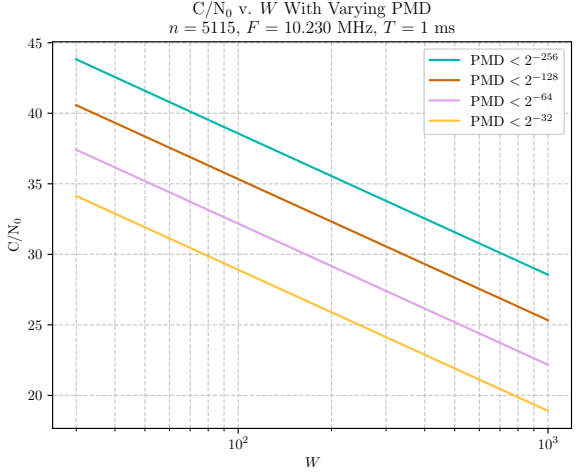
$$\begin{aligned} \text{PMD} \mid \neg\text{SCER} &= \Pr(Y_{\text{PRF},W} \geq 0.5 \mid \neg\text{SCER}) \\ &= \Pr\left(\frac{1}{W} \sum_W (g(B^{-\text{SCER}}) + N_{FT}) \geq 0.5\right) \\ &= \Pr\left(\frac{1}{W} \sum_W g(B^{-\text{SCER}}) + \frac{1}{W} \sum_W N_{FT} \geq 0.5\right) \\ &= \Pr\left(g\left(\frac{1}{W} B^{-\text{SCER},W}\right) + N_{FTW} \geq 0.5\right) \\ &= \sum_b \Pr\left(g\left(\frac{b}{W}\right) + N_{FTW} \geq 0.5\right) \cdot \Pr(b = B^{-\text{SCER},W}) \\ &= \sum_b \text{ccdf}\left(0.5 - g\left(\frac{b}{W}\right)\right) \cdot \Pr(b = B^{-\text{SCER},W}) \quad (21) \end{aligned}$$

Equation (21) provides the exact PMD up the precision of the normal Cumulative Density Function (CDF) and the computational numerical precision.

A. Application to Galileo's E6-C

The Galileo E6-C signal will be used within Galileo's SAS to provide ranging authentication. The E6-C signal utilizes $n = 5115$ ranging codes, and the appropriate Nyquist frequency is $F = 10.230$ MHz. Once encryption is enabled, the ranging code will become a PRF under a commitment-based authentication protocol. Utilizing eq. (21), fig. 2 provides the PMD varying W integrally from 0 to 800. fig. 2 was computed with SciPy utilizing the log survival function (log complimentary CDF function) and the products within the sum of eq. (21) utilizing the log product rule. Each of these steps was to minimize the losses from machine precision.

Several applications utilize Galileo's E6-C PRF sequence to authenticate another band (e.g., E1-B). If the receiver does not

Fig. 3. Minimum Noise Assumptions over Aggregation Time with varying security requirements utilizing the CLT approximations. Results below $W = 30$ are not provided because this figure utilizes the CLT formulations.

track separately the E6-C PRF signal (e.g., via E6-B or via network), local environmental effects may require the receiver to conduct a search to find the correlation peak. For instance, this search could be required on the tracking states (e.g., carrier phase, doppler frequency, ranging code phase). Therefore, that receiver might try multiple times to find the PRF correlation. The net effect on the security model is that the adversary would be allowed multiple attempts to submit a potential forgery over a single range authentication determination. In that case, the minimum PMD should reflect a minimum security level of 128-bits, and so the receiver should aggregate 341 ms of data when making an authentication determination, based on fig. 2.

If the E6-C authentication determination is aided with another signal that can provide accurate tracking states and the receiver is only allowed one attempt to make the authentication determination, then the security level can decrease provided the PMD is acceptable. This would be appropriate if another signal that is perfectly in phase is used to determine the E6-C tracking states, like the E6-B signal. Then 77 ms aggregations are sufficient, like in other similar applications where 32-bit security is acceptable [17].

I expect that receiver guidelines will not recommend the minimum prescriptive boundaries from the previous paragraphs. Instead, I expect that the guidelines will round up to rounder numbers. For instance, from section III-A, 77 ms could become 100 ms, and 341 ms could become 400 ms. If that is the case, then the initial noise assumption could be lowered further. Figure 3 demonstrates these trends utilizing the CLT approximations. Again, once a suitable candidate is found, eq. (21) should be used to bound the PMD and assert authentication security.

IV. HDSCER PRF RANGING SECURITY

The Non-SCER adversary must guess the R^{PPF} , which explains the 50% probabilities in eqs. (13) and (20). But since the HDSCER adversary may measure R^{PPF} before submitting

to the victim receiver, the SCER adversary will have a better-than-50% chance of guessing each chip. Because a better and better HDSER receiving radio will eventually be able to estimate the PRF ranging code chips eventually, this section offload security arguments to authorities who can detect and search for this equipment. Ideally, the needed equipment will be large enough to be easily detected and destroyed. So in this section, I predict the receiving radio equipment required to perform an HDSER spoof.

With the HDSER adversary, the adversary makes a hard decision on each individual chip. Therefore, the math for the HDSER is identical to the Non-SCER, except that the binomial distribution probability p is greater than 50%:

$$B^{\text{HDSER},W} \sim \mathcal{B}(nW, p) ; \quad (22)$$

$$\text{PMD} \mid \text{HDSER} =$$

$$\sum_b \text{ccdf}_{N_{FTW}} \left(0.5 - g \left(\frac{b}{W} \right) \right) \cdot \Pr(b = B^{\text{HDSER},W}) \quad (23)$$

Again, the CLT approximations can be helpful. In that case, eqs. (18) and (19) can be extended:

$$\begin{aligned} \mathbb{E}[Y_{\text{PRF}} \mid \text{HDSER}] &= g(\mathbb{E}[B^{\text{HDSER}}]) \\ &= g(np) ; \end{aligned} \quad (24)$$

$$\mathbb{E}[Y_{\text{PRF}} \mid \text{HDSER}] = 2p - 1 ; \quad (24)$$

$$\mathbb{V}[Y_{\text{PRF}} \mid \text{HDSER}] = \frac{4}{n}p(1-p) + \frac{1}{FT} \cdot \frac{\sigma^2}{P} . \quad (25)$$

A. Application to Galileo's E6-C

This section provides an example application of applying HDSER PRF ranging security to Galileo's E6-C signal. Bounding the HDSER adversary requires assumptions that are ultimately subjective. A better adversarial receiving radio will eventually break the security afforded by any ranging service. So this application, I assume that the HDSER adversary is on the ground receiving the maximum specified power from the Galileo ICD and that the ground temperature is 300 K. From the Galileo E6B/C Code Technical Note, the total received maximum power on the ground for E6-C is -153 dBW, after accounting for the 50% power split to E6-C [18]. Therefore, the precorrelation SNR is about -19 dB for the chip-estimating HDSER adversary.

Figure 4 provides the computed PMD given an adversarial chip-estimating SNR, generated from the CLT formulations from eqs. (24) and (25) and assuming a chip estimation probability from (3) with a receiver C/N_0 of 30 dB. I used the CLT formulations here because of the computational speed and the expected small deviation from eq. (23). An assumed adversarial chip SNR of -19 dB is already breaking 32-bit security. However, given the PMD, it is very probable (i.e., exponentially likely) that the attack would be detected by the receiver after multiple $Y_{\text{PRF},W}$ checks.

An interesting behavior observable from fig. 4 is that once the HDSER adversary is more than 50% likely to submit a forgery, increasing W supports the adversary (hence the vertical order of the W curves reverse in fig. 4 on the right side). The effect of increasing W removes uncertainty from the noise. At this inflection point, the adversary has

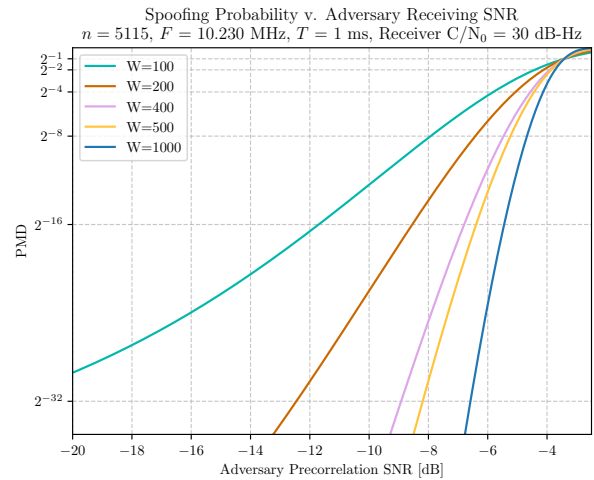


Fig. 4. Comparison of HDSER PMD with multiple W against the adversarial precorrelation chip SNR.

a chip-estimation probability of 75%, which from eq. (24) predicts that the expectation crosses the $Y_{\text{PRF}} = 0.5$ decision boundary. Therefore, at that point, the shrinking noise effect from increasing W makes the adversarial forgery probability better. This occurs when the chip SNR is -3.42 dB after solving eq. (3) with 75% (or when the adversarial gain is about 15.58 dB considering the 300 K assumption).

At this inflection point, the affects of increasing adversarial jamming no longer benefit the adversary. This means our conservative radio model from section I-C is no longer conservative. Increasing either F or the assumed C/N_0 each benefit the adversary (rather than the reverse before). Therefore a conservative radio model would involve a high F and receiver C/N_0 . The net effect of this model's reversal past this inflection point is the adversary will be able to certainly and effectively break the security of the ranging authentication under a conservative radio model. Therefore, once the adversary estimates the chips with sufficient probability that its expectation of the spoofed Y_{PRF} is above the decision boundary, the HDSER completely breaks authentication security.

To counteract this, one can increase the $Y_{\text{PRF}} = 0.5$. But that comes at the expense of the PFA. Figure 5 provides a plot of this trade off. After making a selection at the expense of PFA with fig. 5, fig. 4 must be recalculated using the new decision boundary. Then, after computing an expected antenna gain to break the system, a description of that radio equipment of the systems can be communicated to authorities. Given the results from fig. 4 already predict a radio of 15 dB, this will be directional or phased array antenna that cannot be miniaturized, providing some level of assurance that such equipment could be detected and destroyed.

V. EXPERIMENTAL VALIDATION

To validate the PMDs derived in the previous sections, I perform Monte Carlo experiments. The previous sections, and their application to Galileo's E6-C, are constructed so that the PMD is unreasonable small to provide authentication security.

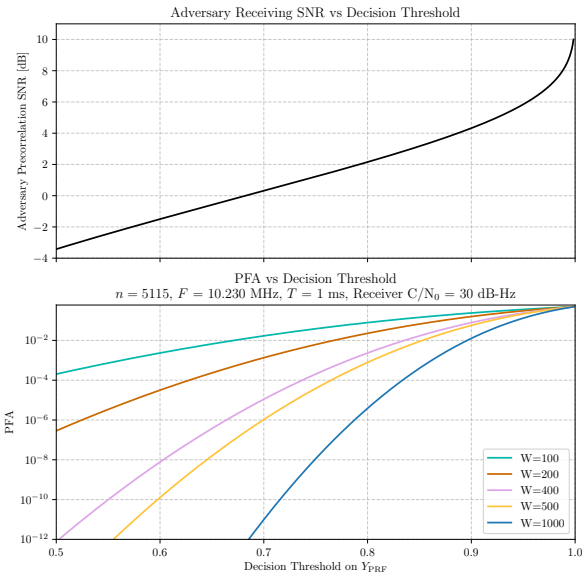


Fig. 5. The effect of increasing decision boundary on Y_{PRF} on the needed breaking Adversarial SNR and PFA.

These design goals pose the same challenge in simulation: an unreasonable number of trials is required to observe a single missed detection. So, in this section, the simulated C/N_0 is decreased substantially so that the mathematical models can actually predict simulated missed detections.

Figure 6 provides the results of a Monte Carlo experiment to verify eq. (21). In the experiment, each trial involves a simulated baseband signal. The authentic and Non-SCER replicas are both chosen randomly and then resampled, with a simulated Non-SCER spoof fed through the simulated receiver filter and threshold-authentication determination. After conducting all the trials, the fraction of observed missed detections forms an estimator of the actual PMD. Figure 6 compares the measured PMD and CLT 99.7% confidence bounds against the predicted PMD. In our implementation, the same function is used to generate figs. 2 and 6. Based on how the experiments match the predictions, I validate eq. (21) and fig. 2.

Figure 7 provides the results of a Monte Carlo experiment to verify eq. (23). In the experiment, each trial involves a simulated baseband signal. The authentic replica is chosen randomly, and then I simulate the HDSCER's ability to estimate the authentic replica chips. Then both replicas are resampled with a simulated HDSCER spoof fed through the simulated receiver filter and threshold-authentication determination. After conducting all the trials, the fraction of observed missed detections forms an estimator of the predicted PMD. Figure 7 compares the measured PMD and CLT 99.7% confidence bounds against the predicted PMD. In our implementation, the same function is used to generate figs. 4 and 7. Based on how the experiments match the predictions, I validate eq. (23) and fig. 4.

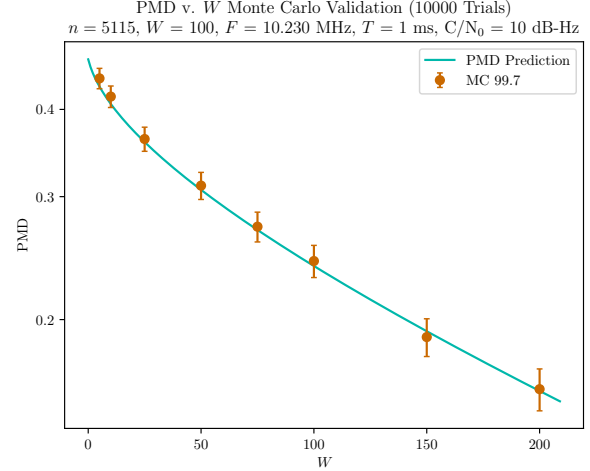


Fig. 6. Monte Carlo results verifying eq. (21)

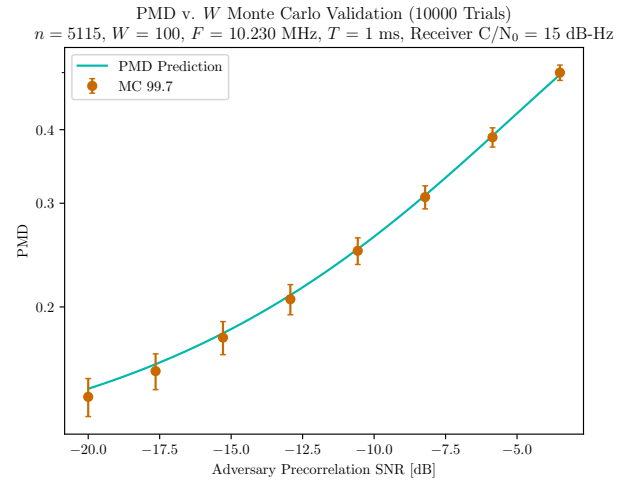


Fig. 7. Monte Carlo results verifying eq. (23)

A. PSCER Soft Information Advantage

While the HDSCER provides a mathematically concise pathway to predict the SCER security probabilities, this section provides simulated evidence of a slightly better SCER adversary. The HDSCER adversary ignores the soft information in its measurement and does not modify its power levels. Here, I define the PSCER adversary that sets the individual chip powers proportional to the measured posterior probability of each chip. But to counteract noticeable effects on the power, the PSCER adversary normalizes its output power over a whole PRF ranging aggregation interval (hence "proportional"). In effect, if the adversary is more certain on a estimated chip, it will provide that chip more power in its spoof. This adversary glosses over many effects, such as the effects of the radio's analog-to-digital gain control; however, the purpose of this section is to simply to show the existence of a better adversary.

Figure 8 provides a simulation showing a small advantage with the PSCER adversary over the HDSCER. Since the PSCER simulated PMD is above the HDSCER PMD, the PSCER has an advantage over the HDSCER. I provide these

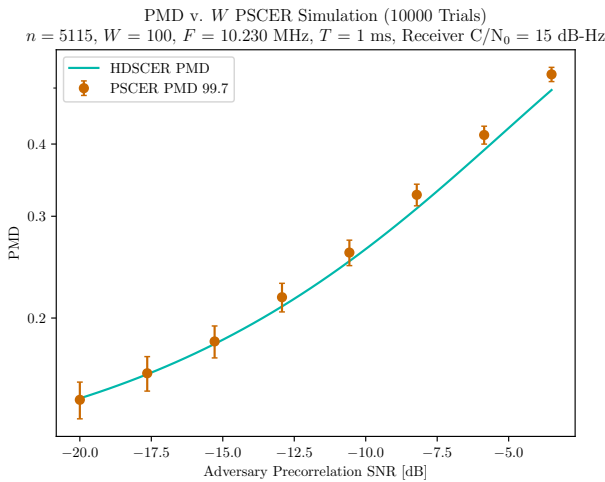


Fig. 8. Simulated Results Demonstrating PSCER Advantage

results to show that some performance improvement can be obtained by utilizing soft information, but not much. Looking at how far left the PSCER line is to the HDSCER line predicts the soft information advantage of approximately 0.6 dB. Therefore, one could account for this result by compensating the adversarial SNR of 0.6 dB within section IV. However, this result still does not provide an upper bound on the potential SCER performance.

VI. CONCLUSION

This work provides derived distributions of the authentication security of PRF GNSS ranging under several adversarial models. With the derivations and predictions of this work, the GNSS designer can design a secure PRF ranging authentication service. Under the Non-SCER model, one can utilize these derivations to specify how long a receiver must correlate PRF ranging codes to provide a specific PMD. Under the HDSCER model, one can predict the needed spoofing radio equipment needed to break authentication security. For Galileo's E6-C, I conclude that a receiver must aggregate at most 100 or 400 ms of PRF Galileo E6-C to assert 32-bit and 128-bit security under Galileo's SAS, respectively. Moreover, I predict that an SCER antenna with a 15 dB gain antenna should be able to estimate the chips sufficiently to break authentication security of Galileo's E6-C PRF signal, neglecting the difficulty in quickly processing, transporting, and transmitting without detection either by a local authority or by the receiver's onboard GNSS-independent clock.

When a receiver utilizes a PRF pseudorange to authenticate another pseudorange, it will apply a pseudorange difference threshold to assert security of the other pseudorange. When the PMD is bounded to standard cryptographic security levels (e.g., 128-bit), under a non-SCER adversarial model, then the pseudorange difference threshold can be relaxed to increase the processes specificity (i.e., decrease PFA) and limit the false alarms resulting from environmental effects. Under the non-SCER model, even when a pseudorange is early or late, the adversary cannot produce a forgery up to the security level.

Therefore, the false alarms resulting from pseudorange delays (e.g., multi path, carrier frequency effects) can be removed by relaxing a pseudorange difference threshold without compromising sensitivity to spoofers.

REFERENCES

- [1] I. Fernandez-Hernandez et al., "Semiassisted signal authentication for galileo: Proof of concept and results," *IEEE Transactions on Aerospace and Electronic Systems*, vol. 59, no. 4, pp. 4393–4404, 2023. DOI: 10.1109/TAES.2023.3243587
- [2] T. A. A. when available, "Testing galileo sas with encrypted signal-in-space," in *Proceedings of the 38th International Technical Meeting of the Satellite Division of The Institute of Navigation (ION GNSS+ 2022)*, 2025, TODO: add page when available.
- [3] J. Anderson, "World's first authenticated satellite pseudorange from orbit," in *Proceedings of the 38th International Technical Meeting of the Satellite Division of The Institute of Navigation (ION GNSS+ 2022)*, 2025, TODO: add page when available.
- [4] L. Scott, "Anti-Spoofing & Authenticated Signal Architectures for Civil Navigation Systems," in *Proceedings of the 16th International Technical Meeting of the Satellite Division of The Institute of Navigation (ION GPS/GNSS 2003)*, 2003, pp. 1543–1552.
- [5] J. M. Anderson et al., "Chips-message robust authentication (chimera) for gps civilian signals," 2017, pp. 2388–2416, ISBN: 9781510853317. DOI: 10.33012/2017.15206
- [6] A. Perrig, D. Song, R. Canetti, J. Tygar, and B. Briscoe, "Timed efficient stream loss-tolerant authentication (tesla): Multicast source authentication transform introduction," *Request For Comments (RFC)*, vol. 4082, 2005.
- [7] Air Force Research Laboratory, "IS-AGT-101: Timed Efficient Stream Loss-tolerant Authentication (TESLA) Chips Message Robust Authentication (Chimera) Enhancement for the L1C Signal: Space Segment/User Segment Interface," Air Force Research Laboratory, Space Vehicles Director, Tech. Rep., 2024.
- [8] J. Anderson, "Designing cryptography systems for gnss data and ranging authentication," Ph.D. dissertation, Stanford University, Dec. 2024.
- [9] J. Anderson, S. Lo, and T. Walter, "Authentication security of combinatorial watermarking for gnss signal authentication," *NAVIGATION: Journal of the Institute of Navigation*, vol. 71, no. 3, 2024, ISSN: 0028-1522. DOI: 10.33012/navi.655 eprint: [https://navi.ion.org/content/71/3/navi.655](https://navi.ion.org/content/71/3/navi.655.full.pdf) [Online]. Available: <https://navi.ion.org/content/71/3/navi.655>
- [10] J. Anderson, S. Lo, and T. Walter, "Combinatorial watermarking under limited scer adversarial models," *NAVIGATION: Journal of the Institute of Navigation*, vol. 72, no. 2, 2025, ISSN: 0028-1522. DOI: 10.33012/navi.696 eprint: <https://navi.ion.org/content/72/2/navi.696.full.pdf> [Online]. Available: <https://navi.ion.org/content/72/2/navi.696>

- [11] T. A. A. when available, “range authentication of galileo e1 / e5 signals using different assisted methods on a gnss hardware receiver,” in *Proceedings of the 38th International Technical Meeting of the Satellite Division of The Institute of Navigation (ION GNSS+ 2022)*, 2025, TODO: add page when available.
- [12] M. L. Psiaki and T. E. Humphreys, “Gnss spoofing and detection,” *Proceedings of the IEEE*, vol. 104, no. 6, pp. 1258–1270, 2016. DOI: 10.1109/JPROC.2016.2526658
- [13] C. O’Driscoll, T. Scuccato, A. DallaChiara, T. Pany, M. Diez, and M. Hameed, *The Attack Agnostic Defence: a Spoofing Detection Metric for Secure Spreading Sequences*, 2022.
- [14] I. Fernandez-Hernandez et al., “Galileo signal authentication service (sas),” in *Proceedings of the 37th International Technical Meeting of the Satellite Division of The Institute of Navigation (ION GNSS+ 2024)*, 2024, pp. 3292–3307.
- [15] R. T. Gallego, “Analysis and implementation of anti-spoofing detection methods based on galileo signal authentication service,” *TDX (Tesis Doctorals en Xarxa)*, Nov. 2024. [Online]. Available: <http://www.tdx.cat/handle/10803/693183>
- [16] J. Anderson, S. Lo, and T. Walter, “Time synchronization of tesla-enabled gnss receivers,” *IEEE Transactions on Aerospace and Electronic Systems*, vol. 61, no. 4, pp. 9550–9566, 2025. DOI: 10.1109/TAES.2025.3552074
- [17] J. Anderson, S. Lo, A. Neish, and T. Walter, “Authentication of satellite-based augmentation systems with over-the-air rekeying schemes,” *NAVIGATION: Journal of the Institute of Navigation*, vol. 70, no. 3, 2023, ISSN: 0028-1522. DOI: 10.33012/navi.595 [Online]. Available: <https://navi.ion.org/content/70/3/navi.595>
- [18] EUSPA, “Galileo e6-b/c codes technical note,” vol. 1, Jan. 2019.